0013-7227/08/$15.00/0
Printed in U.S.A.

Endocrinology 149(8):3890–3899
Copyright © 2008 by The Endocrine Society
doi: 10.1210/en.2008-0140

Notch Inhibits Osteoblast Differentiation and Causes Osteopenia

Stefano Zanotti, Anna Smerdel-Ramoya, Lisa Stadmeyer, Deena Durant, Freddy Radtke, and Ernesto Canalis

Department of Research (S.Z., A.S.-R., L.S., D.D., E.C.), Saint Francis Hospital and Medical Center, Hartford, Connecticut 06105; University of Connecticut School of Medicine (A.S.-R., E.C.), Farmington, Connecticut 06030; and Swiss Institute for Experimental Cancer Research (F.R.), CH-1066 Epalinges, Switzerland

Notch receptors are determinants of cell fate decisions. To define the role of Notch in the adult skeleton, we created transgenic mice overexpressing the Notch intracellular domain (NICD) under the control of the type I collagen promoter. First-generation transgenics were small and osteopenic. Bone histomorphometry revealed that NICD caused a decrease in bone volume, secondary to a reduction in trabecular number; osteoblast and osteoclast number were decreased. Low fertility of founder mice and lethality of young pups did not allow the complete establishment of transgenic lines. To characterize the effect of Notch overexpression *in vitro*, NICD was induced in osteoblasts and stromal cells from *Rosa*^{notch} mice, in which a STOP cassette flanked by *lox*^{P} sites is upstream of NICD, by transduction with an adenoviral vector expressing Cre recombinase (Cre) under the control of the cytomegalovirus (CMV) promoter (Ad-CMV-Cre). NICD impaired osteoblastogenesis and inhibited Wnt/β-catenin signaling. To determine the effects of *notch1* deletion *in vivo*, mice in which *notch1* was flanked by *lox*^{P} sequences (*notch1*$^{loxP/loxP}$) were mated with mice expressing Cre recombinase under the control of the osteocalcin promoter. Conditional null *notch1* mice had no obvious skeletal phenotype, possibly because of rescue by *notch2*; however, 1-month-old females exhibited a modest increase in osteoclast surface and eroded surface. Osteoblasts from *notch1*$^{loxP/loxP}$ mice, transduced with Ad-CMV-Cre and transfected with Notch2 small interfering RNA, displayed increased alkaline phosphatase activity. In conclusion, Notch signaling in osteoblasts causes osteopenia and impairs osteoblastogenesis by inhibiting the Wnt/β-catenin pathway. (*Endocrinology* 149: 3890–3899, 2008)

NOTCH PLAYS A critical role in cell fate decisions, and in mammals it regulates neural crest (1) and vascular (2) development and plays a critical role during somitogenesis (3). Notch also contributes to the regulation of tissue renewal in the intestine (4), skin (5), hematopoietic system (6), and mammary epithelium (7). There are four Notch receptors (Notch1–4) and seven known ligands, which are Serrate/Jagged1 and 2; Delta Like1, 3, and 4 (8); Delta/Notch-like epidermal growth factor-related receptor (9); and contactin/F3/NB-3 (10). Receptors and ligands are single-pass transmembrane proteins expressed on the surface of adjacent cells. In the canonical Notch signaling pathway, Notch-ligand interactions result in the proteolytic cleavage of the extracellular region of Notch by a disintegrin and metalloproteinase domain metalloproteases, and in the subsequent cleavage within the transmembrane region of Notch by γ-secretase (11). Proteolysis results in the release of the Notch intracellular domain (NICD), which translocates to the nucleus (12, 13), in which it interacts with members of the Epstein-Barr virus latency C promoter binding factor 1, suppressor of hairless and lag-1 (CSL) family of transcription factors. This interaction converts the CSL proteins from transcriptional repressors to transcriptional activators (14), inducing the expression of hairy enhancer of split (HES) 1 or 5 (15, 16) and HES-related repressor proteins 1–3 (17).

Wnt can activate three distinct signaling pathways, but in osteoblasts the Wnt/β-catenin canonical pathway is used (18, 19). In the absence of Wnt, axin, adenomatous polyposis coli, β-catenin, and glycogen synthase kinase (GSK)-3β form a complex in which β-catenin is phosphorylated by casein kinase-1α and GSK3β, leading to β-catenin degradation after ubiquitination (20). Activation of the canonical Wnt pathway leads to the inhibition of GSK3β and the stabilization and nuclear translocation of β-catenin. In the nucleus, β-catenin associates with members of the lymphoid enhancer binding factor-1/T cell-specific factor-4 family of transcription factors and regulates gene transcription (21–23). Activation of Notch and Wnt canonical signaling pathways plays an important role in osteoblastogenesis. Notch and Wnt pathways interact at different levels, and Notch often, but not always, opposes Wnt/β-catenin signaling (24–30).

Mesenchymal cells can differentiate into cells of various lineages, including osteoblasts, myoblasts, chondrocytes, and adipocytes (31). The fate of mesenchymal cells and their differentiation toward cells of the osteoblastic lineage is tightly controlled by a network of extracellular and intra-

First Published Online April 17, 2008

Abbreviations: Ad, Adenovirus; APA, alkaline phosphatase activity; BMP, bone morphogenetic protein; CMV, cytomegalovirus; Cre, Cre recombinase; CSL, Epstein-Barr virus latency C promoter binding factor 1/suppressor of hairless/lag 1; FBS, fetal bovine serum; FVB, tropism to friend leukemia virus strain B; GAPDH, glyceraldehyde-3-phosphate dehydrogenase; GFP, green fluorescent protein; GSK, glycogen synthase kinase; HES, hairy enhancer of split; NICD, Notch intracellular domain; Oc-Cre, Cre recombinase under the control of a human osteocalcin promoter; RPL38, ribosomal protein L38; siRNA, small interfering RNA; Smad, signaling mother against decapentaplegic; WT, wild type.

***Endocrinology* is published monthly by The Endocrine Society (http://www.endo-society.org), the foremost professional society serving the endocrine community.**

The Endocrine Society. Downloaded from press.endocrine.org by [${individualUser.displayName}] on 21 January 2014. at 08:24 For personal use only. No other uses without permission. . All rights reserved.

cellular signals, such as bone morphogenetic proteins, Wnt/β-catenin, and Notch (19, 32). We reported that forced and constitutive expression of NICD in ST-2 stromal and MC3T3 osteoblastic cells suppresses osteoblastic differentiation (33) by inhibiting Wnt/β-catenin signaling (34). However, some controversy on the effect of Notch on osteoblastic maturation exists, and both inhibitory (35, 36) and stimulatory (37, 38) effects on osteoblast differentiation and function have been reported. Deletion of *notch1*, *-2*, and *-3* in osteoclast precursors enhances osteoclastogenesis and bone resorption, indicating an inhibitory role of Notch on osteoclastogenesis (36).

The intent of this study was to define the function of Notch signaling in skeletal tissue *in vivo* and *in vitro*. For this purpose, we created transgenic mice overexpressing NICD under the control of the osteoblast-specific 3.6-kb rat collagen type I promoter and determined their skeletal phenotype. An osteoblast-specific conditional deletion approach, to ablate *notch1* in the adult bone environment, was also used, by crossing mice, in which *notch1* sequences were flanked by lox^P sites ($notch1^{loxP/loxP}$), with transgenic mice expressing the Cre recombinase (Cre) under the control of the osteocalcin promoter. The *in vivo* phenotype and the phenotype of cells obtained from mice misexpressing Notch1 were examined.

Materials and Methods

Transgenic and conditional null mice

The 2.3-kb fragment coding for the murine NICD was cloned downstream of the 3.6-kb rat type I collagen promoter (39). Microinjection of linearized DNA into pronuclei of fertilized oocytes from tropism to friend leukemia virus strain B (FVB) inbred mice (Charles River Laboratories, Wilmington, MA), and transfer of microinjected embryos into pseudopregnant mice were carried out at the Transgenic Facility of the University of Connecticut Health Center (Farmington, CT). Positive founders were identified by Southern blot analysis of tail DNA (40) and bred to wild-type FVB mice for the generation of hemizygous mice.

Transgenic $Rosa^{notch}$ mice, created in a hybrid 129/C57BL/6 genetic background, were obtained from D. A. Melton (Harvard University, Cambridge, MA) (41). In these mice, the *Rosa26* locus is targeted with a DNA construct encoding NICD, followed by an internal ribosome entry sequence and nuclear-localized enhanced green fluorescent protein (GFP) and preceded by a STOP cassette flanked by lox^P sites. Constitutive expression of NICD from the targeted *Rosa26* locus is induced after the deletion of the STOP cassette by Cre recombination of lox^P sequences.

For the creation of a conditional *notch1* null deletion, the *notch1* locus was targeted for lox^P modification, as described (42) to obtain $notch1^{loxP/loxP}$ mice, which were propagated in a C57BL/6 genetic background. Cre recombination in these mice results in the removal of a 3.5-kb segment of the putative promoter of *notch1* and part of the first exon encoding its signal peptide. Transgenic FVB inbred mice expressing the Cre recombinase under the control of a 3.9-kb human osteocalcin promoter (Oc-Cre) were obtained from T. Clemens (University of Alabama, Birmingham, AL) (43). Oc-Cre mice were mated to $notch1^{loxP/loxP}$ mice, and the progeny intermated to obtain heterozygous Oc-Cre mice in a homozygous $notch1^{loxP/loxP}$ background ($notch1^{loxP/loxP}$:*Oc-Cre*$^{+/-}$). These mice were intermated, generating an experimental cohort, in which Cre deletes the lox^P-flanked sequences from the $notch1^{loxP}$ alleles ($notch1^{D/D}$) and a control littermate cohort lacking the Cre recombinase allele ($notch1^{loxP/loxP}$). To ensure that the latter were appropriate controls, wild-type (WT) mice were compared with $notch1^{loxP/loxP}$ littermates for their skeletal phenotype. Male and female mice were compared with littermate controls of the same sex at 3 or 4 wk of age, a time of marked expression of the osteocalcin gene. Deletion of lox^P-flanked sequences by the Cre recombinase was documented by PCR in DNA extracted from calvariae of 4-wk-old mice using the forward primer 5′-CTGACTTAGGGGGAAAAC-3′ and the reverse primer 5′-TAAAAAGCGACAGCTGCGGAG-3′ to create a 470-bp product. Animal experiments were approved by the Animal Care and Use Committee of Saint Francis Hospital and Medical Center.

X-ray analysis and bone histomorphometric analysis

Radiography was performed on killed 2-wk-old NICD transgenic mice on a Faxitron x-ray system (model MX 20; Faxitron x-ray Corp., Wheeling, IL). The x-rays were performed at an intensity of 30 kV for 20 sec. Static histomorphometry was carried out on femurs from experimental and control mice killed by CO_2 inhalation. Femurs were dissected, fixed in 70% ethanol, dehydrated, and embedded undecalcified in methyl methacrylate. Longitudinal sections, 5 μm thick, were cut on a microtome (Microm; Richard-Allan Scientific, Kalamazoo, MI) and stained with 0.1% toluidine blue (pH 6.4) or Von Kossa. Static parameters of bone formation and resorption were measured in a defined area between 725 and 1270 μm from the growth plate, using an OsteoMeasure morphometry system (Osteometrics, Atlanta, GA). The terminology and units used are those recommended by the Histomorphometry Nomenclature Committee of the American Society for Bone and Mineral Research (44).

Cell cultures and adenoviral infection

Osteoblasts were isolated from parietal bones of 3- to 5-d-old $Rosa^{notch}$ or $notch1^{loxP/loxP}$ mice by sequential collagenase digestion, as described (45). Cells were cultured in DMEM (Invitrogen, Carlsbad, CA) supplemented with nonessential amino acids, 20 mM HEPES, 100 μg/ml ascorbic acid, and 10% fetal bovine serum (FBS; Atlanta Biologicals, Norcross, GA) at 37 C in a humidified 5% CO_2 incubator. Bone marrow stromal cells were recovered by centrifugation of femurs that were aseptically removed from 4-wk-old $Rosa^{notch}$ mice, as described (46). Cells were plated at a density of 5×10^5 cells/cm^2 and cultured in α-MEM (Invitrogen) containing 15% FBS at 37 C in a humidified 5% CO_2 incubator.

At subconfluence, stromal cells or osteoblasts were transferred to either α-MEM or DMEM containing 2% FBS for 1 h before exposure overnight to 100 multiplicity of infection of replication defective recombinant adenoviruses (Ad). To induce recombination of the lox^P sequences, an adenoviral vector expressing Cre recombinase under the control of the cytomegalovirus (CMV) promoter (Ad-CMV-Cre) (Vector Biolabs, Philadelphia, PA) was transduced. An adenoviral vector expressing GFP under the control of the CMV promoter (Ad-CMV-GFP) (Vector Biolabs) was used as a control. Cells were washed in versene (Invitrogen), and stromal cells or osteoblasts were cultured in the presence of either α-MEM or DMEM containing 10% FBS. Recombination of lox^P sequences was tested by Southern blot analysis in $Rosa^{notch}$ cell cultures.

RNA interference

To down-regulate Notch2 expression *in vitro*, a 19-mer double-stranded small interfering (si) RNA targeted to bp 1965–1983 of the Notch2 mouse mRNA sequence was obtained commercially, and a scrambled 19-mer siRNA with no homology to known mouse or rat sequences was used as control (Ambion, Austin, TX) (47, 48). Notch2 or scrambled siRNA, both at 20 nM, was transfected into subconfluent $notch1^{loxP/loxP}$ osteoblasts after transduction with Ad-CMV-GFP or Ad-CMV-Cre to delete *notch1*, using siLentFect lipid reagent, in accordance with the manufacturer's instructions (Bio-Rad, Hercules, CA). Cells were allowed to recover for 24 h before the determination of alkaline phosphatase activity (APA). To ensure adequate down-regulation, total RNA was extracted in parallel cell cultures 96 h after the transfection of siRNAs and Notch2 mRNA levels determined by real time RT-PCR.

APA

To determine the effects of Notch1 on APA, $Rosa^{notch}$ stromal cells and osteoblasts or $notch1^{loxP/loxP}$ osteoblasts, transduced with Ad-CMV-GFP or Ad-CMV-Cre, were cultured in the presence of 100 μg/ml ascorbic acid and 5 mM β-glycerophosphate (Sigma-Aldrich, St. Louis, MO) and treated with recombinant bone morphogenetic protein (BMP)-2 (Wyeth, Collegeville, PA) or Wnt 3a (R&D Systems, Minneapolis, MN) for 72 h and harvested. APA was determined in 0.5% Triton X-100 cell extracts

The Endocrine Society. Downloaded from press.endocrine.org by [${individualUser.displayName}] on 21 January 2014. at 08:24 For personal use only. No other uses without permission. . All rights reserved.

by the hydrolysis of *p*-nitrophenyl phosphate to *p*-nitrophenol and measured by spectroscopy at 405 nm after 10 min of incubation at room temperature, according to the manufacturer's instructions (Sigma-Aldrich). Data are expressed as nanomoles of *p*-nitrophenol released per minute per microgram of protein. Total protein content was determined in cell extracts by the DC protein assay, in accordance with the manufacturer's instructions (Bio-Rad).

Real-time RT-PCR

Total RNA was extracted from cell cultures after transduction with Ad-CMV-GFP or Ad-CMV-Cre and mRNA levels determined by real-time RT-PCR (49, 50). For this purpose, 5 μg of total RNA were reverse transcribed using SuperScript III platinum two-step quantitative RT-PCR kit (Invitrogen), according to the manufacturer's instructions and amplified in the presence of 5′-CGGTTAGGGCGTCTCCACAGTAAC-[FAM]G-3′ and 5′-CTTGGAGAGGGCCACAAAGG-3′ primers for alkaline phosphatase; 5′-TCCAGGAGTTAAGTGATTTGCTCA-3′ and 5′-CGAAGTTACATGACACTGGGCTT[FAM]G-3′ primers for glyceraldehyde-3-phosphate dehydrogenase (GAPDH); 5′-GACTTTCACGGCCTCT-GAGCACAGAAAG[FAM]C-3′ and 5′-ATTCTTGCCCTTCGCCTCTT-3′ primers for HES1; 5′-GAACTGCCCATGACCACTACCCAGTT[FAM]C-3′ and 5′-GGGTGTTGTCCACAGGTGA-3′ primers for Notch1; 5′-CGGCTGT-TGATGAGTGTATCTCCAGC[FAM]G-3′ and 5′-GTAGCTGCCCTGAGT-GTTGTGG-3′ primers for Notch2; 5′-CACTTACGGCGCTACCTTGGGTA-AGT[FAM]G-3′ and 5′-CCCAGCACAACTCCTCCCTA-3′ primers for osteocalcin; and 5′-CGAACCGGATAATGTGAAGTTCAAGGTT[FAM]G-3′ and 5′-CTGCTTCAGCTTCTCTGCCTTT-3′ primers for ribosomal protein L38 (RPL38) and platinum quantitative PCR SuperMix-UDG (Invitrogen) at 60 C for 45 cycles. Gene copy number was estimated by comparison with a standard curve constructed using osteocalcin (J. B. Lian, University of Massachusetts, Worcester, MA) (51), alkaline phosphatase, and HES1 (both from American Type Culture Collection, Manassas, VA) cDNAs and corrected for *gapdh* (R. Wu, Cornell University, Ithaca, NY) copy number in *Rosa*^{notch} stromal cells or *notch1*$^{loxP/loxP}$ osteoblasts (52) or *rpl38* (53) (American Type Culture Collection) in *Rosa*^{notch} osteoblasts. Reactions were conducted in a 96-well spectrofluorometric thermal iCycler (Bio-Rad), and fluorescence was monitored during every PCR cycle at the annealing step.

Western blot analysis

To assess the effects of NICD overexpression on cytosolic β-catenin levels or signaling mother against decapentaplegic (Smad) 1/5/8 phosphorylation, *Rosa*^{notch} stromal cells, after transduction with Ad-CMV-GFP or Ad-CMV-Cre, were serum deprived overnight and exposed to control medium, Wnt 3a for 16 h, or BMP-2 for 20 min. To determine cytosolic β-catenin levels, the cell layer was washed in PBS and extracted in 10 mM Tris, 140 mM NaCl, 5 mM EDTA, and 2 mM dithiothreitol buffer (pH 7.6) in the presence of protease inhibitors and the cytosolic fraction separated by ultracentrifugation, as described (54). Twenty micrograms of total cytosolic protein were fractionated by gel electrophoresis in 7.5% polyacrylamide gels and transferred to Immobilon P membranes (Millipore, Billerica, MA). The membranes were blocked with 3% BSA in PBS and exposed to a 1:500 dilution of a monoclonal antibody to unphosphorylated β-catenin (Santa Cruz Biotechnology, Santa Cruz, CA) or exposed to a 1:1000 dilution of a goat polyclonal antibody to actin (Santa Cruz Biotechnology). To determine the level of Smad 1/5/8 phosphorylation, the cell layer was washed in PBS and extracted in cell lysis buffer (Cell Signaling Technology, Beverly, MA) in the presence of protease and phosphatase inhibitors. Protein concentrations were determined using a DC protein assay kit (Bio-Rad), and 20 μg of total cellular protein were fractionated by electrophoresis in 10% polyacrylamide gels and transferred to Immobilon P membranes. The membranes were blocked with 3% BSA in PBS and exposed to a rabbit polyclonal antibody, which recognizes Smad 1/5/8 phosphorylated at carboxyl-terminal serine residues (Cell Signaling Technology) or exposed to a mouse monoclonal antibody to unphosphorylated Smad 1 (Santa Cruz Biotechnology) at a 1:1000 dilution. All blots were exposed to antirabbit or antimouse IgG antiserum conjugated to horseradish peroxidase and developed with a chemiluminescence detection reagent (PerkinElmer, Waltham, MA).

Transient transfections

To determine changes in Notch signaling in *Rosa*^{notch}, calvarial osteoblasts, transduced with Ad-CMV-Cre or Ad-CMV-GFP, were transfected with a construct containing six multimerized dimeric CSL binding sites, linked to the β-globin basal promoter (12xCSL-Luc; L. J. Strobl, Institute for Clinical Molecular Biology, Munich, Germany), or a 354-bp fragment of the HES1 promoter (HES1-Luc; U. Lendahl, Karolinska Institute, Stockholm, Sweden), both cloned upstream of the *luciferase* reporter gene (55–58). Transient transfections were conducted in *Rosa*^{notch} osteoblasts cultured to 70% confluence using FuGene6 (3 μl FuGene6/2 μg DNA), according to the manufacturer's instructions (Roche, Indianapolis, IN). A CMV-directed β-galactosidase expression construct (CLONTECH, San Jose, CA) was used to control for transfection efficiency. Cells were exposed to the FuGENE6-DNA mix for 16 h, transferred to α-MEM containing 10% FBS for 24 h, and harvested. Luciferase and β-galactosidase activities were measured using an Optocomp luminometer (MGM Instruments, Hamden, CT). Luciferase activity was corrected for β-galactosidase activity.

Statistical analysis

Data are expressed as means ± SEM. Statistical differences were determined by ANOVA or Student's *t* test.

Results

Type I collagen transgenic mice

Three founder mice overexpressing NICD under the control of the 3.6-kb rat type I collagen promoter were identified. One founder had a total of five litters, but none of the born pups carried the transgene. A second founder had only one litter containing two pups carrying the transgene, and both died unexpectedly at 2 wk of age. A third founder had five litters and a total of four mice carried the transgene, which died between 3 and 4 wk of age but were available for analysis. Because of the early death of NICD transgenics, appropriate transgenic lines could not be established. However, we were able to perform a limited number of observations on the hemizygous mice available. Hemizygous NICD transgenic mice were compared with WT littermate controls at 3–4 wk of age. Contact radiography of the skeleton revealed that transgenic mice were smaller than WT controls and appeared osteopenic (Fig. 1A). Bone histomorphometric analysis of distal femurs from 3- to 4-wk-old hemizygous NICD transgenics revealed an 80% decrease in bone volume per tissue volume, due to a reduced number of trabeculae (Table 1 and Fig. 1B). The observed decrease in bone volume was associated with a reduction in the number of osteoblasts per tissue area, number of osteoblasts per bone perimeter, and osteoblast surface per bone surface (Table 1 and Fig. 1C). Although the number of osteoclasts per tissue area was decreased because of the lesser number of trabeculae, the number of osteoclasts per bone perimeter and osteoclast surface per bone surface were not different from controls (Table 1).

NICD overexpression in vitro

Because the founder mice and the first generation of NICD transgenics died before the establishment of transgenic lines, the impact of NICD overexpression on osteoblastic cell function was investigated in cells from *Rosa*^{notch} mice, in which a STOP cassette, between the *Rosa26* promoter and the NICD coding sequence, is flanked by *lox*^{P} sites. Bone marrow stromal cells and calvarial osteoblasts from *Rosa*^{notch} mice were

The Endocrine Society. Downloaded from press.endocrine.org by [${individualUser.displayName}] on 21 January 2014. at 08:24 For personal use only. No other uses without permission. . All rights reserved.

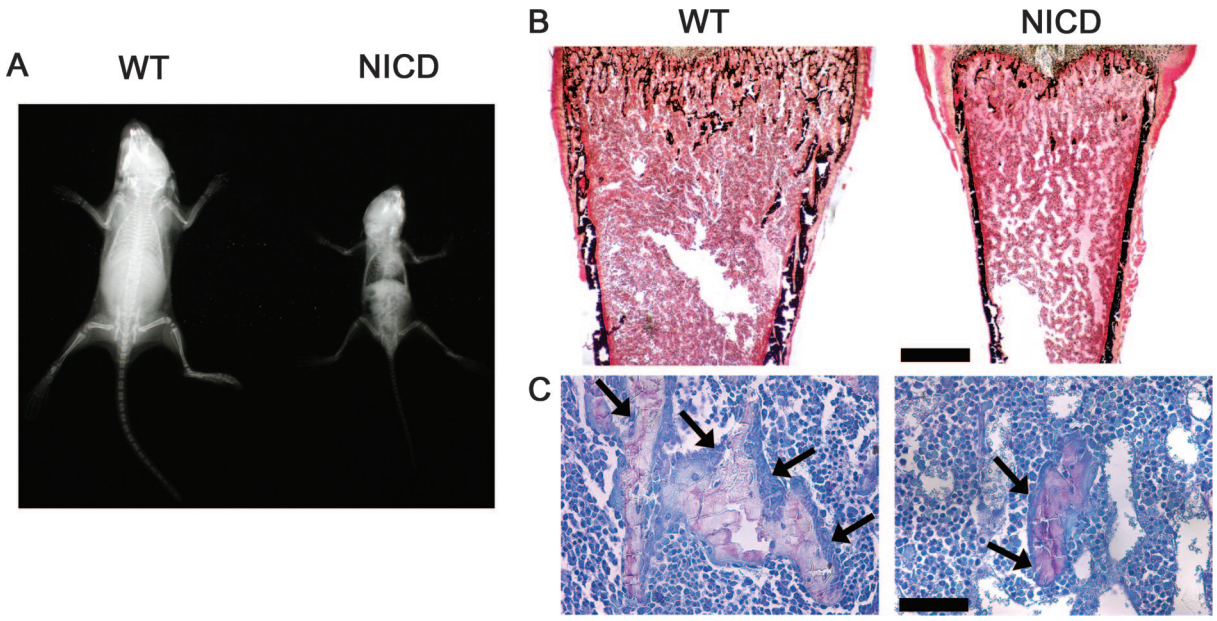

FIG. 1. Phenotype of NICD-overexpressing mice. A, Representative skeletal radiograph of a 4-wk-old WT control and a NICD transgenic mouse. B and C, Representative bone histomorphometry performed on femurs from 4-wk-old WT control and NICD transgenic mice stained with Von Kossa (B) and toluidine blue (C). Final magnifications, ×40 (B) and ×400 (C). *Bars*, 400 μm (B) and 40 μm (C). *Arrows* point to osteoblasts.

cultured and transduced with an adenoviral vector expressing recombinant Cre under the control of the CMV promoter (Ad-CMV-Cre) to induce NICD expression or with a control vector in which the CMV promoter drives the expression of GFP (Ad-CMV-GFP). Effective recombination of lox^P sequences and removal of the STOP cassette was documented by Southern blot analysis of cellular DNA; recombination was detected in cells transduced with Ad-CMV-Cre and not in control cells transduced with Ad-CMV-GFP (Fig. 2A). Confirming the overexpression of Notch, $Rosa^{notch}$ stromal cells transduced with Ad-CMV-Cre expressed Notch1 transcripts that were 6-fold greater than that in Ad-CMV-GFP-transduced cells (Fig. 2C). Accordingly, Ad-CMV-Cre-transduced cells expressed mRNA levels of the Notch target *hes1* that were 16-fold greater than in Ad-CMV-GFP transduced cells. After 3 d of culture, NICD-overexpressing cultures exhibited suppressed APA. Furthermore, Notch decreased the stimulatory effects of BMP-2 and Wnt 3a on APA (Fig. 2B). Accordingly, alkaline phosphatase and osteocalcin mRNA levels were suppressed in $Rosa^{notch}$ marrow stromal cells overexpressing NICD, confirming its inhibitory effect on osteoblastic differentiation (Fig. 2C). To examine possible mechanisms underlying the decreased osteoblastic differentiation in Ad-CMV-Cre transduced $Rosa^{notch}$ stromal cells, we tested whether NICD overexpression affected BMP/Smad or Wnt/β-catenin signaling. Confirming previous studies (34), BMP-2 induced Smad 1/5/8 phosphorylation, but NICD overexpression did not modify the effect of BMP-2 on Smad 1/5/8 phosphorylation (not shown), whereas NICD overexpression decreased the levels of cytosolic β-catenin and opposed the stimulatory effect of Wnt 3a on cytosolic β-catenin levels (Fig. 2D).

TABLE 1. Femoral static histomorphometry of 3- to 4-wk-old NICD transgenic mice and WT controls

	WT	NICD
Bone volume/tissue volume (%)	8.6 ± 2.1	1.5 ± 0.4[a]
Trabecular separation (μm)	135.5 ± 47.8	336.6 ± 18.2[a]
Trabecular number (mm^{-1})	9.2 ± 1.8	2.4 ± 0.6[a]
Trabecular thickness (μm)	8.7 ± 0.8	6.5 ± 0.4
Osteoblast surface/bone surface (%)	31.9 ± 6.0	9.9 ± 2.2[a]
Number of osteoblasts/bone perimeter (mm^{-1})	67.1 ± 12.1	21.1 ± 4.5[a]
Number of osteoblasts/tissue area (mm^{-2})	832.1 ± 89.0	74.1 ± 31.6[a]
Osteoclast surface/bone surface (%)	12.0 ± 0.6	12.8 ± 0.8
Number of osteoclasts/bone perimeter (mm^{-1})	12.3 ± 0.5	12.0 ± 1.3
Number of osteoclasts/tissue area (mm^{-2})	182.0 ± 40.2	39.2 ± 10.6[a]
Eroded surface/bone surface (%)	22.4 ± 1.6	22.7 ± 4.5

Bone histomorphometry was performed on femurs from 3- to 4-wk-old NICD hemizygous mice and littermate WT controls. Values are pooled from three litters and are expressed as means ± SEM; n = 4–5.

[a] Significantly different from WT controls, $P < 0.05$.

In preliminary experiments, we were unable to transfect reporter constructs with sufficient efficiency into bone marrow stromal cells. Consequently, to perform these experiments and confirm the results observed in stromal cells, calvarial osteoblasts from $Rosa^{notch}$ mice were isolated and transduced with Ad-CMV-Cre to induce NICD overexpression or with Ad-CMV-GFP to be used as control. Cre recombination of lox^P sequences was confirmed by Southern blot analysis (Fig. 3A); Notch1 overexpression was confirmed by real-time RT-PCR, and Notch1 transcripts were 2.5-fold greater in Ad-CMV-Cre transduced cells than that in control Ad-CMV-GFP cells (Fig. 3D). To confirm the activation of Notch signaling, cells were transfected with a 12xCSL-Luc Notch reporter construct or with HES1-Luc, a fragment

The Endocrine Society. Downloaded from press.endocrine.org by [${individualUser.displayName}] on 21 January 2014. at 08:24 For personal use only. No other uses without permission. . All rights reserved.

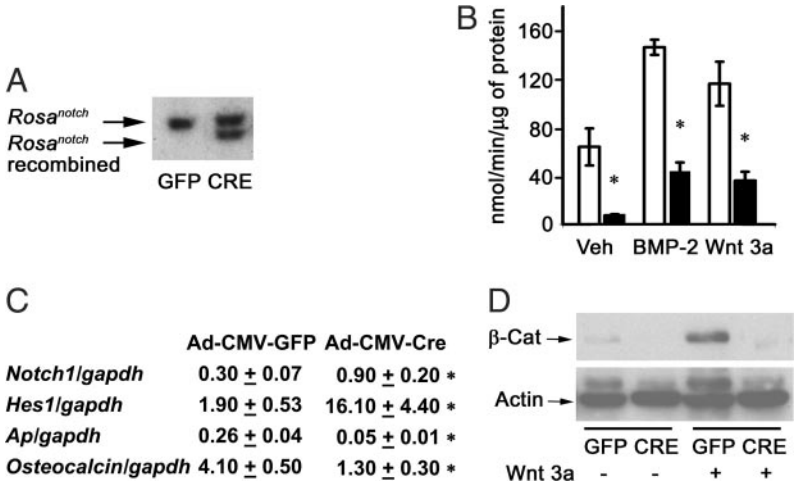

FIG. 2. Effect of NICD overexpression on osteoblastic differentiation in bone marrow stromal cells harvested from *Rosa*^{notch} mice and transduced with Ad-CMV-GFP or Ad-CMV-Cre. A, Stromal cells were cultured for 3 d after confluence and examined for *lox*^{P} recombination by Southern blot analysis. B, Stromal cells were cultured to confluence, exposed to control medium (Veh), BMP-2 at 3 nM, or Wnt 3a at 2.7 nM for 72 h and APA quantified in extracts from cells transduced with control Ad-CMV-GFP (*white bars*) or Ad-CMV-Cre (*black bars*). APA is expressed as nanomoles of *p*-nitrophenol per minute per microgram of total protein. *Bars*, means ± SEM for six observations. *, Significantly different from control cells, $P < 0.05$. C, Stromal cells transduced with control Ad-CMV-GFP or Ad-CMV-Cre were cultured to confluence; total RNA was reverse transcribed and amplified by real-time RT-PCR in the presence of specific primers. Data are expressed as *notch1*, *hes1, alkaline phosphatase (Ap)*, and *osteocalcin* copy number, determined by real-time RT-PCR, corrected for *gapdh* expression. Values are means ± SEM, n = 3. *, Significantly different from control cells, $P < 0.05$. D, Stromal cells were cultured to confluence, serum deprived overnight, and treated 16 h with Wnt 3a at 2.7 nM (+) or control vehicle (−) for the determination of cytosolic β-catenin levels. Cytosolic extracts were resolved by gel electrophoresis and transferred to Immobilon P membranes, which were incubated with antibodies to β-catenin (β-cat) or actin.

of the HES1 promoter driving the expression of *luciferase*. Ad-CMV-Cre transduced cells induced the transactivation of 12xCSL-Luc and of HES1-Luc reporter constructs, compared with control cells (Fig. 3B), indicating activation of the canonical Notch signaling pathway. In accordance with the results obtained in stromal cells from *Rosa*^{notch} mice, calvarial

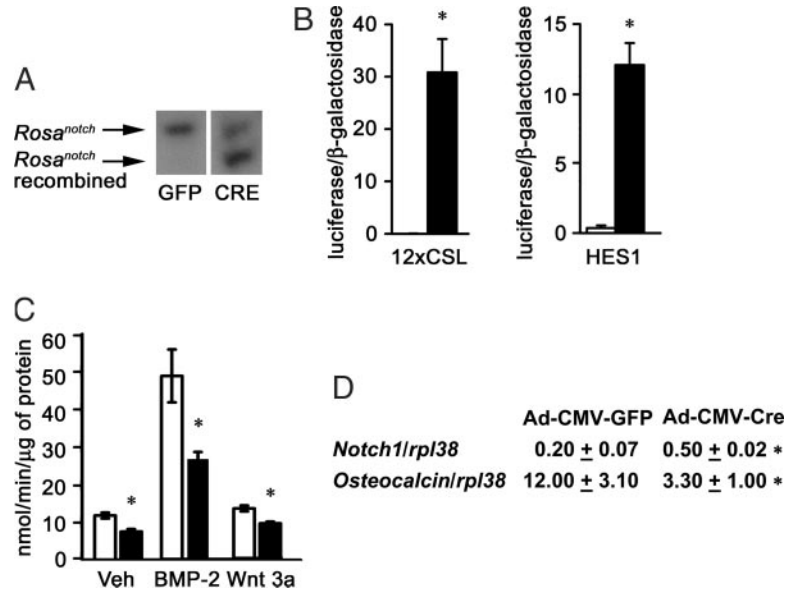

FIG. 3. Effect of NICD overexpression on osteoblastic differentiation in calvarial osteoblasts harvested from *Rosa*^{notch} mice and transduced with Ad-CMV-GFP or Ad-CMV-Cre. A, Calvarial osteoblasts were cultured for 3 d after confluence and examined for *lox*^{P} recombination by Southern blot analysis. B, Calvarial osteoblasts were cultured to 70% confluence and transfected with 12xCSL-Luc, HES1-Luc, and a CMV/β-galactosidase expression vector. After 16 h, cells were switched to fresh DMEM for 24 h and harvested. Data shown represent luciferase/β-galactosidase activity for control Ad-CMV-GFP cells (*white bars*) or Ad-CMV-Cre (*black bars*). *Bars*, means ± SEM for six observations. *, Significantly different from control cells, $P < 0.05$. C, Calvarial osteoblasts were cultured to confluence; exposed to control medium (Veh), BMP-2 at 3 nM, or Wnt 3a at 2.7 nM for 72 h; and APA quantified in extracts from cells transduced with Ad-CMV-GFP cells (*white bars*) or Ad-CMV-Cre (*black bars*). APA is expressed as nanomoles of *p*-nitrophenol per minute per microgram of total protein. *Bars*, Means ± SEM for six observations. *, Significantly different from control cells, $P < 0.05$. D, Calvarial osteoblasts transduced with Ad-CMV-GFP or Ad-CMV-Cre were cultured to confluence; total RNA was reverse transcribed, and amplified by real-time RT-PCR in the presence of specific primers. Data are expressed as *notch1* and *osteocalcin* copy number, determined by real-time RT-PCR, and corrected for *rpl38* expression. Values are means ± SEM, n = 4. *, Significantly different from control cells, $P < 0.05$.

The Endocrine Society. Downloaded from press.endocrine.org by [${individualUser.displayName}] on 21 January 2014. at 08:24 For personal use only. No other uses without permission. . All rights reserved.

TABLE 2. Femoral static histomorphometry of 4-wk-old *notch1*$^{loxP/loxP}$ female mice and WT female littermate controls

	WT	*Notch1*$^{loxP/loxP}$
Bone volume/tissue volume (%)	10.6 ± 1.6	10.0 ± 1.0
Trabecular separation (μm)	123.6 ± 20.5	118.7 ± 8.7
Trabecular number (mm^{-1})	8.4 ± 1.1	7.8 ± 0.5
Trabecular thickness (μm)	12.4 ± 0.6	12.7 ± 0.5
Osteoblast surface/bone surface (%)	25.3 ± 0.9	25.3 ± 2.3
Number of osteoblasts/bone perimeter (mm^{-1})	45.4 ± 2.0	46.0 ± 4.1
Number of osteoblasts/tissue area (mm^{-2})	607.0 ± 86.4	574.4 ± 76.0
Osteoclast surface/bone surface (%)	9.5 ± 0.6	9.0 ± 0.7
Number of osteoclasts/bone perimeter (mm^{-1})	8.4 ± 0.5	7.8 ± 0.6
Number of osteoclasts/tissue area (mm^{-2})	110.0 ± 14.1	95.4 ± 7.6
Eroded surface/bone surface (%)	23.5 ± 1.7	24.7 ± 1.9

Bone histomorphometry was performed on femurs from 4-wk-old *notch1*$^{loxP/loxP}$ female mice and WT littermate controls. Values are means ± SEM; n = 7.

osteoblasts overexpressing Notch1 exhibited decreased levels of APA when compared with control cells cultured with vehicle, BMP-2, or Wnt 3a (Fig. 3C). Osteocalcin mRNA levels were decreased in Ad-CMV-Cre-transduced osteoblasts (Fig. 3D), confirming that NICD overexpression impairs osteoblastic differentiation.

Notch1 conditional null mice

Bone histomorphometry revealed that *notch1*$^{loxP/loxP}$ homozygous mice were not different from WT littermate controls (Table 2), indicating that the presence of *lox*^{P} sequences did not cause a skeletal phenotype. Thus, *notch1*$^{loxP/loxP}$ mice were considered appropriate controls for the conditional *notch1* null mice (*notch1*$^{\Delta/\Delta}$). The mating scheme involved intercrossing heterozygous osteocalcin Cre transgenics in a homozygous *notch1*$^{loxP/loxP}$ background (*notch1*$^{loxP/loxP}$*: Oc-Cre*$^{+/-}$). To monitor for the absence of *notch1* in bone tissue, deletion of *notch1* sequences flanked by *lox*^{P} sites was documented by PCR in DNA extracted from calvariae of 4-wk-old mice. Deletion of the *lox*^{P}-flanked region was detected in calvarial extracts from the experimental cohort, *notch1*$^{\Delta/\Delta}$, whereas no recombination was observed in extracts from littermate *notch1*$^{loxP/loxP}$ controls (Fig. 4A). Bone histomorphometric analysis of femurs from 4-wk-old female *notch1*$^{\Delta/\Delta}$ revealed that they were not different from controls (Table 3 and Fig. 4B), except for an increase in eroded surface per bone surface and osteoclast surface per bone surface; a nonsignificant increase in osteoclast number per perimeter and per area was also noted (Table 3). Four-week-old male *notch1*$^{\Delta/\Delta}$ mice did not exhibit a skeletal phenotype when compared with *notch1*$^{loxP/loxP}$ male littermate controls (not shown).

Notch1 deletion in vitro

We hypothesized that the lack of a phenotype in *notch1*$^{\Delta/\Delta}$ mice was secondary to the rescue of Notch activity by *notch2*. Because a double *notch1*, *notch2* conditional null mouse was not readily available to our laboratory at the time the studies were conducted, Notch2 expression was down-regulated *in vitro* in the context of the *notch1* deletion to assess the function of Notch in osteoblasts. *Notch1*$^{loxP/loxP}$ calvarial osteoblasts were transduced with Ad-CMV-Cre to ablate *notch1* expression, whereas *notch2* was down-regulated by RNA interference. The expression of Notch1 and Notch2 mRNA was suppressed in these cells (Fig. 5A). *Notch1*$^{loxP/loxP}$ calvarial osteoblasts transduced with Ad-CMV-Cre and transfected with Notch2 siRNA exhibited increased levels of APA after treatment with BMP-2, Wnt 3a, or control vehicle, compared with Ad-CMV-GFP-transduced cells transfected with scrambled siRNA (Fig. 5B). Thus, removal of Notch signaling *in vitro* causes an increase in APA in calvarial osteoblasts, which is in accordance with the suppressive effects of NICD overexpression on APA observed in *Rosa*^{notch} calvarial osteoblasts and stromal cells.

Discussion

Our results demonstrate that transgenic mice overexpressing NICD under the control of the 3.6-kb rat type I collagen pro-

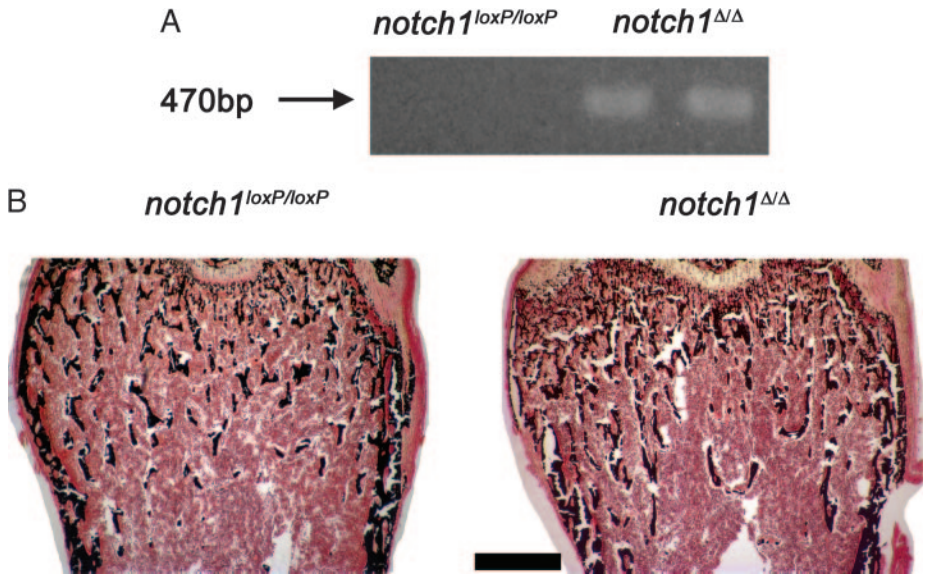

FIG. 4. Phenotype of conditional null *notch1*$^{\Delta/\Delta}$ 4-wk-old female mice. A, Representative PCR analysis of calvarial DNA from conditional null *notch1*$^{\Delta/\Delta}$ 4-wk-old mice and *notch1*$^{loxP/loxP}$ littermate control mice. B, Von Kossa staining performed on femurs from 4-wk-old *notch1*$^{\Delta/\Delta}$ female mice and *notch1*$^{loxP/loxP}$ female littermate controls. Final magnification, ×40. *Bar*, 400 μm.

The Endocrine Society. Downloaded from press.endocrine.org by [${individualUser.displayName}] on 21 January 2014. at 08:24 For personal use only. No other uses without permission. . All rights reserved.

TABLE 3. Femoral static histomorphometry of 4-wk-old *notch1*$^{\Delta/\Delta}$ female mice and *notch1*$^{loxP/loxP}$ female littermate controls

	Notch1$^{loxP/loxP}$	*Notch1*$^{\Delta/\Delta}$
Bone volume/tissue volume (%)	7.8 ± 1.2	8.5 ± 0.5
Trabecular separation (μm)	174.8 ± 60.2	116.5 ± 3.8
Trabecular number (mm^{-1})	7.1 ± 1.1	7.9 ± 0.3
Trabecular thickness (μm)	11.1 ± 0.3	10.9 ± 0.7
Osteoblast surface/bone surface (%)	26.4 ± 3.0	22.9 ± 2.9
Number of osteoblasts/bone perimeter (mm^{-1})	50.2 ± 4.8	44.6 ± 5.7
Number of osteoblasts/tissue area (mm^{-2})	526.4 ± 75.1	555.5 ± 78.2
Osteoclast surface/bone surface (%)	12.7 ± 0.7	15.8 ± 1.1[a]
Number of osteoclasts/bone perimeter (mm^{-1})	12.0 ± 0.7	14.7 ± 1.1
Number of osteoclasts/tissue area (mm^{-2})	130.8 ± 19.9	181.0 ± 10.7
Eroded surface/bone surface (%)	25.1 ± 1.1	31.9 ± 1.9[a]

Bone histomorphometry was performed on femurs from 4-wk-old *notch1*$^{\Delta/\Delta}$ female mice and *notch1*$^{loxP/loxP}$ littermate controls. Values are means ± SEM; n = 5.

[a] Significantly different from *notch1*$^{loxP/loxP}$ controls, $P < 0.05$.

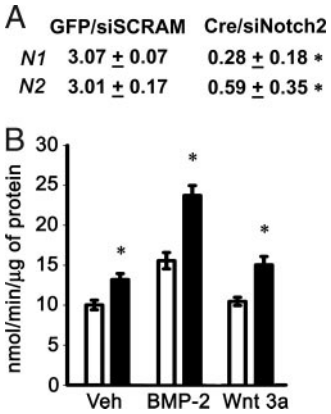

FIG. 5. Effect of Notch signaling inhibition on osteoblastic differentiation in calvarial osteoblasts harvested from *notch1*$^{loxP/loxP}$ mice transduced with Ad-CMV-GFP or Ad-CMV-Cre and transfected with Notch2 siRNA. Transduced osteoblasts were cultured to 70% confluence, and transfected with Notch2 (siNotch2) or control scrambled siRNA (siSCRAM). A, Deletion of Notch1 and down-regulation of Notch2 mRNA were documented in parallel cultures by real-time RT-PCR at the completion of the experiment. Data are expressed as *notch1 (N1)* and *notch2 (N2)* copy number, determined by real-time RT-PCR, corrected for *gapdh* expression. Values represent means ± SEM for three observations. *, Significantly different from control cells, $P < 0.05$. B, Ad-CMV-GFP-transduced cells were transiently transfected with scrambled siRNA (*white bars*) and used as controls, whereas Ad-CMV-Cre-transduced cells were transiently transfected with notch2 siRNA (*black bars*). Twenty-four hours after transfection, cells were exposed to control medium (Veh), BMP-2 at 3 nM, or Wnt 3a at 2.7 nM and APA quantified in extracts from cells cultured for 72 h. APA is expressed as nanomoles of *p*-nitrophenol per minute per microgram of total protein. *Bars*, means ± SEM for six observations. *, Significantly different from control cells, $P < 0.05$.

moter exhibit osteopenia and impaired growth when compared with control WT mice of the same age and genetic composition. The decrease in bone volume and trabecular number appears to be secondary to a decrease in osteoblast number. This is possibly secondary to an inhibition of cell differentiation caused by Notch, which would maintain cells of the osteoblastic lineage in an undifferentiated state. An increase in apoptosis could cause a decrease in osteoblast number, but no increase in cell death was detected in femoral sections of Notch transgenics when examined by the terminal uridine deoxynucleotidyl transferase deoxyuridine 5-triphosphate nick end labeling reaction (data not shown). Regrettably, the early death of NICD transgenics precluded the full establishment of a transgenic line and the study of dynamic parameters of bone histomorphometry.

We suspect intrauterine lethality of NICD transgenics because only six transgenics were born from 11 litters. The cause of the intrauterine loss was not established, but if embryonic death occurred, it could have been related to a developmental impact of Notch in nonskeletal tissues (1–3). The 3.6-kb type I collagen promoter is activated at d 14 of embryonic life, and its expression is not entirely specific to skeletal cells (39). Although this fragment of the type I collagen promoter is commonly used for the study of gene expression in osteoblastic cells and the skeletal phenotype of Notch transgenics is pronounced, one cannot exclude that the impaired growth observed in Notch1 transgenics is due to a runting effect or nonspecific effects secondary to Notch expression in various connective tissues. Recently impaired osteoblast maturation was reported in transgenics in which NICD expression was under the control of a 2.3-kb fragment of the type I collagen promoter (59). Lethality was not reported when Notch was expressed under the control of the 2.3-kb type I collagen fragment, possibly because this fragment is less active and more specific to osteoblasts than the 3.6-kb type I collagen fragment (39). It is of interest that 2.3-kb type I collagen NICD transgenics showed increased bone volume, and the tissue was composed of immature woven bone, secondary to the presence of immature osteoblasts (59). The differences in the phenotypes reported can be explained by the differential activation of the 2.3- and 3.6-kb fragment of the type I collagen promoter, resulting in the arrest of osteoblastic cell differentiation at different stages of maturation (39). It is possible that NICD overexpression under the control of the 2.3-kb type I collagen promoter represses the terminal differentiation of osteoblasts and allows for the proliferation of immature cells, leading to the increased formation of woven bone and the reported phenotype (59). In contrast, NICD overexpression under the control of the 3.6-kb type I collagen promoter would repress osteoblastogenesis at an earlier stage of cell differentiation, leading to a decreased number of mature osteoblasts and an osteopenic phenotype.

Expression of Notch1 under the control of the osteocalcin promoter was attempted to determine Notch activity in mature osteoblasts, but mice exhibited newborn lethality secondary to hydrocephalus, most likely due to osteocalcin expression and Notch activation in the central nervous system (60). Postnatal activation of NICD in mature osteoblasts using *Rosa*^{notch} was attempted by mating *Rosa*^{notch} mice with mice expressing a tamoxifen inducible Cre estrogen receptor type 2 fusion protein, under the control of the 2.3-kb type I collagen promoter (61). However, the administration of tamoxifen inhibited bone turnover and reduced osteoblast and osteoclast number, eroded surface, and bone formation, thereby obscuring a potential Notch phenotype (data not shown).

The conditional deletion of *notch1* in mature osteoblasts *in vivo* did not cause an obvious skeletal phenotype. This could

The Endocrine Society. Downloaded from press.endocrine.org by [${individualUser.displayName}] on 21 January 2014. at 08:24 For personal use only. No other uses without permission. . All rights reserved.

be due to the rescue of *notch1* function by its paralogue *notch2* because both genes are expressed in primary rodent (62) and human osteoblasts (63). It is also possible that the expression of the Cre recombinase under the control of the osteocalcin promoter deleted *notch1* in mature osteoblasts, whereas Notch1 appears to target the differentiation of immature cells of the osteoblastic lineage and may not affect the function of terminally differentiated cells. A recent report from another laboratory described the use of the *prx1* enhancer to express Cre in the limb primordia and delete both *notch1* and *notch2* in the developing skeleton (64). This approach proved effective because it targeted less differentiated cells, caused elongation of the hypertrophic cartilage region, and increased trabecular bone mass. The data are consistent with the results reported in the present paper on Notch transgenics. It is important to note that the conditional deletion of *notch1* caused an increase in eroded surface and osteoclast surface per bone surface, even if the effect was small and observed only in female mice; this result confirms previous observations establishing that Notch inhibits osteoclastogenesis (36).

Because we were unable to establish a transgenic line overexpressing NICD, we considered the use of *Rosa*^{notch} mice as an alternate source of bone marrow stromal cells and calvarial osteoblasts for mechanistic studies *in vitro*. In *Rosa*^{notch} cells, NICD expression can be induced after the adenoviral transduction of Cre recombinase to delete the STOP cassette upstream of the NICD coding sequence. The findings in cells from *Rosa*^{notch} mice are in accordance with the results from transgenic mice overexpressing NICD and previous work on the effects of Notch in cell lines. The transduction of retroviral vectors to overexpress NICD in ST-2 stromal and MC3T3 osteoblastic cell lines demonstrated that Notch signaling inhibits the expression of osteoblastic gene markers and caused a reduction in mineralized nodule formation (33), indicating an inhibition of osteoblastogenesis. Accordingly, NICD overexpression in primary cultures of stromal cells and calvarial osteoblasts from *Rosa*^{notch} mice caused a suppression of APA and a reduction in osteocalcin mRNA levels. Conversely, *in vitro* experiments in calvarial osteoblasts in conditions of *notch1* and *notch2* suppression caused an increase in APA. The observation confirms studies in mammalian nonskeletal cells, in which NICD interacts with runt-related transcription factor-2 and represses the transactivation of an osteocalcin reporter construct (59, 64).

Our findings corroborate the notion, proposed in previous studies by our group and others (33–36), that Notch inhibits osteoblastogenesis. However, transient stimulation of Notch signaling can sensitize osteoblastic cell lines to selected effects of BMP-2 (37, 38), and interference with Notch activity by the use of a γ-secretase inhibitor prevents a stimulatory effect of BMP-2 on APA in MC3T3 osteoblastic cells (37). The exact reason for the discrepancies is not clear, although they could be explained by the use of different cells, time of cellular exposure to Notch, and experimental approaches. Notch could play a dual stimulatory and inhibitory role during osteoblastogenesis. A dual role for Notch has been proposed in the chondrogenic differentiation of human bone marrow stromal cells, in which Notch signal activation induced by Jagged1 is necessary for the early phases of chondrogenesis, but Jagged1 needs to be down-regulated to allow for differentiation to continue (65).

Although Notch increased *hes1* transcript levels and *hes1* promoter activity in calvarial osteoblasts, other Notch target genes may be responsible for the effect of Notch on osteoblastogenesis. Further investigations are needed to clarify the role of HES1 in osteoblastogenesis because the effects of HES1 do not always recapitulate those of Notch in cells of mesenchymal origin (66). Furthermore, different targets of Notch signaling could be involved in mediating the effects of Notch on osteoblastogenesis, and HES-related repressor proteins 2, an alternate Notch effector, is known to inhibit osteoblastic differentiation (35). In addition, there is evidence of Notch autoregulation in bone marrow stromal cells and calvarial osteoblasts. NICD overexpression in cells from *Rosa*^{notch} mice caused a 50–90% suppression of Notch2 mRNA levels (data not shown). This could represent down-regulation of *notch2* by *notch1* or possibly a negative feedback loop leading to a generalized suppression of Notch expression after the activation of the Notch signaling cascade. As expected, Notch1 mRNA levels were not repressed because its transcription was under the control of the *Rosa26* promoter.

In previous work, we have shown that NICD overexpression inhibits osteoblastogenesis by opposing canonical Wnt/β-catenin signaling (34). These results were confirmed in bone marrow stromal cells from *Rosa*^{notch} mice overexpressing NICD, which exhibited reduced basal and Wnt 3a-induced cytosolic β-catenin levels. Because the canonical Wnt signaling pathway is necessary for bone development and the regulation of bone mass (19), the opposing action of Notch on this pathway supports the role of Notch signaling as a suppressor of osteoblastogenesis. These observations are in accordance with studies in nonosteoblastic cells, demonstrating cross talk between Notch and Wnt pathways (24–30).

In conclusion, our results demonstrate that Notch inhibits osteoblastogenesis, causing osteopenia, possibly by inhibiting the Wnt/β-catenin pathway.

Acknowledgments

The authors thank Drs. D. A. Melton for the *Rosa*^{notch} mice, T. Clemens for the Cre transgenic mice, and B. de Crombrugghe for the Cre estrogen receptor type mice; L. J. Strobl for 12xCSL-Luc reporter construct and U. Lendahl for HES1-Luc promoter construct; J. B. Lian for osteocalcin cDNA and R. Wu for GAPDH cDNA; Wyeth Research for BMP-2; and M. Burton and T. X. Le for technical help.

Received January 30, 2008. Accepted April 4, 2008.

Address all correspondence and requests for reprints to: Ernesto Canalis, M.D., Department of Research, Saint Francis Hospital and Medical Center, 114 Woodland Street, Hartford, Connecticut 06105-1299. E-mail: ecanalis@stfranciscare.org.

This work was supported by Grant DK045227 from the National Institute of Diabetes and Digestive and Kidney Diseases.

Disclosure Statement: The authors have nothing to disclose.

References

1. **Cornell RA, Eisen JS** 2005 Notch in the pathway: the roles of Notch signaling in neural crest development. Semin Cell Dev Biol 16:663–672
2. **Gridley T** 2007 Notch signaling in vascular development and physiology. Development 134:2709–2718
3. **Gridley T** 2006 The long and short of it: somite formation in mice. Dev Dyn 235:2330–2336
4. **van Es JH, van Gijn ME, Riccio O, van den BM, Vooijs M, Begthel H,**

The Endocrine Society. Downloaded from press.endocrine.org by [${individualUser.displayName}] on 21 January 2014. at 08:24 For personal use only. No other uses without permission. . All rights reserved.

Cozijnsen M, Robine S, Winton DJ, Radtke F, Clevers H 2005 Notch/γ-secretase inhibition turns proliferative cells in intestinal crypts and adenomas into goblet cells. Nature 435:959–963
5. **Lee J, Basak JM, Demehri S, Kopan R** 2007 Bi-compartmental communication contributes to the opposite proliferative behavior of Notch1-deficient hair follicle and epidermal keratinocytes. Development 134:2795–2806
6. **Duncan AW, Rattis FM, DiMascio LN, Congdon KL, Pazianos G, Zhao C, Yoon K, Cook JM, Willert K, Gaiano N, Reya T** 2005 Integration of Notch and Wnt signaling in hematopoietic stem cell maintenance. Nat Immunol 6:314–322
7. **Callahan R, Egan SE** 2004 Notch signaling in mammary development and oncogenesis. J Mammary Gland Biol Neoplasia 9:145–163
8. **Lindsell CE, Boulter J, diSibio G, Gossler A, Weinmaster G** 1996 Expression patterns of Jagged, Δ1, Notch1, Notch2, and Notch3 genes identify ligand-receptor pairs that may function in neural development. Mol Cell Neurosci 8:14–27
9. **Eiraku M, Hirata Y, Takeshima H, Hirano T, Kengaku M** 2002 Δ/Notch-like epidermal growth factor (EGF)-related receptor, a novel EGF-like repeat-containing protein targeted to dendrites of developing and adult central nervous system neurons. J Biol Chem 277:25400–25407
10. **Hu QD, Ang BT, Karsak M, Hu WP, Cui XY, Duka T, Takeda Y, Chia W, Sankar N, Ng YK, Ling EA, Maciag T, Small D, Trifonova R, Kopan R, Okano H, Nakafuku M, Chiba S, Hirai H, Aster JC, Schachner M, Pallen CJ, Watanabe K, Xiao ZC** 2003 F3/contactin acts as a functional ligand for Notch during oligodendrocyte maturation. Cell 115:163–175
11. **Ehebauer M, Hayward P, Martinez-Arias A** 2006 Notch signaling pathway. Sci STKE 2006:cm7
12. **Schroeter EH, Kisslinger JA, Kopan R** 1998 Notch-1 signalling requires ligand-induced proteolytic release of intracellular domain. Nature 393:382–386
13. **Song W, Nadeau P, Yuan M, Yang X, Shen J, Yankner BA** 1999 Proteolytic release and nuclear translocation of Notch-1 are induced by presenilin-1 and impaired by pathogenic presenilin-1 mutations. Proc Natl Acad Sci USA 96:6959–6963
14. **Lai EC** 2002 Keeping a good pathway down: transcriptional repression of Notch pathway target genes by CSL proteins. EMBO Rep 3:840–845
15. **Artavanis-Tsakonas S, Rand MD, Lake RJ** 1999 Notch signaling: cell fate control and signal integration in development. Science 284:770–776
16. **Ohtsuka T, Ishibashi M, Gradwohl G, Nakanishi S, Guillemot F, Kageyama R** 1999 Hes1 and Hes5 as notch effectors in mammalian neuronal differentiation. EMBO J 18:2196–2207
17. **Iso T, Sartorelli V, Poizat C, Iezzi S, Wu HY, Chung G, Kedes L, Hamamori Y** 2001 HERP, a novel heterodimer partner of HES/E(spl) in Notch signaling. Mol Cell Biol 21:6080–6089
18. **Chen AE, Ginty DD, Fan CM** 2005 Protein kinase A signalling via CREB controls myogenesis induced by Wnt proteins. Nature 433:317–322
19. **Westendorf JJ, Kahler RA, Schroeder TM** 2004 Wnt signaling in osteoblasts and bone diseases. Gene 341:19–39
20. **Liu C, Li Y, Semenov M, Han C, Baeg GH, Tan Y, Zhang Z, Lin X, He X** 2002 Control of β-catenin phosphorylation/degradation by a dual-kinase mechanism. Cell 108:837–847
21. **Dale TC** 1998 Signal transduction by the Wnt family of ligands. Biochem J 329(Pt 2):209–223
22. **Gumbiner BM** 1998 Propagation and localization of Wnt signaling. Curr Opin Genet Dev 8:430–435
23. **Wodarz A, Nusse R** 1998 Mechanisms of Wnt signaling in development. Annu Rev Cell Dev Biol 14:59–88
24. **Axelrod JD, Matsuno K, Artavanis-Tsakonas S, Perrimon N** 1996 Interaction between Wingless and Notch signaling pathways mediated by dishevelled. Science 271:1826–1832
25. **De SB, Annaert W** 2001 Where Notch and Wnt signaling meet. The presenilin hub. J Cell Biol 152:F17–F20
26. **Espinosa L, Ingles-Esteve J, Aguilera C, Bigas A** 2003 Phosphorylation by glycogen synthase kinase-3β downregulates Notch activity: a link for notch and Wnt pathways. J Biol Chem 278:32227–32235
27. **Foltz DR, Santiago MC, Berechid BE, Nye JS** 2002 Glycogen synthase kinase-3β modulates notch signaling and stability. Curr Biol 12:1006–1011
28. **Noll E, Medina M, Hartley D, Zhou J, Perrimon N, Kosik KS** 2000 Presenilin affects arm/β-catenin localization and function in Drosophila. Dev Biol 227:450–464
29. **Soriano S, Kang DE, Fu M, Pestell R, Chevallier N, Zheng H, Koo EH** 2001 Presenilin 1 negatively regulates β-catenin/T cell factor/lymphoid enhancer factor-1 signaling independently of β-amyloid precursor protein and notch processing. J Cell Biol 152:785–794
30. **Wesley CS** 1999 Notch and wingless regulate expression of cuticle patterning genes. Mol Cell Biol 19:5743–5758
31. **Bianco P, Gehron RP** 2000 Marrow stromal stem cells. J Clin Invest 105:1663–1668
32. **Canalis E, Deregowski V, Pereira RC, Gazzerro E** 2005 Signals that determine the fate of osteoblastic cells. J Endocrinol Invest 28:3–7
33. **Sciaudone M, Gazzerro E, Priest L, Delany AM, Canalis E** 2003 Notch 1 impairs osteoblastic cell differentiation. Endocrinology 144:5631–5639
34. **Deregowski V, Gazzerro E, Priest L, Rydziel S, Canalis E** 2006 Notch 1 overexpression inhibits osteoblastogenesis by suppressing Wnt/β-catenin but not bone morphogenetic protein signaling. J Biol Chem 281:6203–6210
35. **Zamurovic N, Cappellen D, Rohner D, Susa M** 2004 Coordinated activation of notch, Wnt, and transforming growth factor-β signaling pathways in bone morphogenic protein 2-induced osteogenesis. Notch target gene Hey1 inhibits mineralization and Runx2 transcriptional activity. J Biol Chem 279:37704–37715
36. **Bai S, Kopan R, Zou W, Hilton MJ, Ong CT, Long F, Ross FP, Teitelbaum SL** 2007 Notch1 regulates osteoclastogenesis directly in osteoclast precursors and indirectly via osteoblast lineage cells. J Biol Chem 283:6509–6518
37. **Nobta M, Tsukazaki T, Shibata Y, Xin C, Moriishi T, Sakano S, Shindo H, Yamaguchi A** 2005 Critical regulation of bone morphogenetic protein-induced osteoblastic differentiation by Δ1/Jagged1-activated Notch1 signaling. J Biol Chem 280:15842–15848
38. **Tezuka K, Yasuda M, Watanabe N, Morimura N, Kuroda K, Miyatani S, Hozumi N** 2002 Stimulation of osteoblastic cell differentiation by Notch. J Bone Miner Res 17:231–239
39. **Kalajzic I, Kalajzic Z, Kaliterna M, Gronowicz G, Clark SH, Lichtler AC, Rowe D** 2002 Use of type I collagen green fluorescent protein transgenes to identify subpopulations of cells at different stages of the osteoblast lineage. J Bone Miner Res 17:15–25
40. **Irwin N** 1989 Molecular cloning. In: Femt J, ed. Sambrook. New York: Cold Spring Harbor Laboratory Press; 9.32–9.36
41. **Murtaugh LC, Stanger BZ, Kwan KM, Melton DA** 2003 Notch signaling controls multiple steps of pancreatic differentiation. Proc Natl Acad Sci USA 100:14920–14925
42. **Radtke F, Wilson A, Stark G, Bauer M, van Meerwijk J, MacDonald HR, Aguet M** 1999 Deficient T cell fate specification in mice with an induced inactivation of Notch1. Immunity 10:547–558
43. **Zhang M, Xuan S, Bouxsein ML, von Stechow D, Akeno N, Faugere MC, Malluche H, Zhao G, Rosen CJ, Efstratiadis A, Clemens TL** 2002 Osteoblast-specific knockout of the insulin-like growth factor (IGF) receptor gene reveals an essential role of IGF signaling in bone matrix mineralization. J Biol Chem 277:44005–44012
44. **Parfitt AM, Drezner MK, Glorieux FH, Kanis JA, Malluche H, Meunier PJ, Ott SM, Recker RR** 1987 Bone histomorphometry: standardization of nomenclature, symbols, and units. Report of the ASBMR Histomorphometry Nomenclature Committee. J Bone Miner Res 2:595–610
45. **McCarthy TL, Centrella M, Canalis E** 1990 Cyclic AMP induces insulin-like growth factor I synthesis in osteoblast-enriched cultures. J Biol Chem 265:15353–15356
46. **Gazzerro E, Pereira RC, Jorgetti V, Olson S, Economides AN, Canalis E** 2005 Skeletal overexpression of gremlin impairs bone formation and causes osteopenia. Endocrinology 146:655–665
47. **Sharp PA** 2001 RNA interference—2001. Genes Dev 15:485–490
48. **Elbashir SM, Harborth J, Lendeckel W, Yalcin A, Weber K, Tuschl T** 2001 Duplexes of 21-nucleotide RNAs mediate RNA interference in cultured mammalian cells. Nature 411:494–498
49. **Nazarenko I, Pires R, Lowe B, Obaidy M, Rashtchian A** 2002 Effect of primary and secondary structure of oligodeoxyribonucleotides on the fluorescent properties of conjugated dyes. Nucleic Acids Res 30:2089–2195
50. **Nazarenko I, Lowe B, Darfler M, Ikonomi P, Schuster D, Rashtchian** 2002 A multiplex quantitative PCR using self-quenched primers labeled with a single fluorophore. Nucleic Acids Res 30:e37
51. **Lian J, Stewart C, Puchacz E, Mackowiak S, Shalhoub V, Collart D, Zambetti G, Stein G** 1989 Structure of the rat osteocalcin gene and regulation of vitamin D-dependent expression. Proc Natl Acad Sci USA 86:1143–1147
52. **Tso JY, Sun XH, Kao TH, Reece KS, Wu R** 1985 Isolation and characterization of rat and human glyceraldehyde-3-phosphate dehydrogenase cDNAs: genomic complexity and molecular evolution of the gene. Nucleic Acids Res 13:2485–2502
53. **Kouadjo KE, Nishida Y, Cadrin-Girard JF, Yoshioka M, St. Amand J** 2007 Housekeeping and tissue-specific genes in mouse tissues. BMC Genomics 8:127
54. **Young CS, Kitamura M, Hardy S, Kitajewski J** 1998 Wnt-1 induces growth, cytosolic β-catenin, and Tcf/Lef transcriptional activation in rat-1 fibroblasts. Mol Cell Biol 18:2474–2485
55. **Nam Y, Sliz P, Song L, Aster JC, Blacklow SC** 2006 Structural basis for cooperativity in recruitment of MAML coactivators to Notch transcription complexes. Cell 124:973–983
56. **Wilson JJ, Kovall RA** 2006 Crystal structure of the CSL-Notch-Mastermind ternary complex bound to DNA. Cell 124:985–996
57. **Strobl LJ, Hofelmayr H, Stein C, Marschall G, Brielmeier M, Laux G, Bornkamm GW, Zimber-Strobl U** 1997 Both Epstein-Barr viral nuclear antigen 2 (EBNA2) and activated Notch1 transactivate genes by interacting with the cellular protein RBP-Jκ. Immunobiology 198:299–306
58. **Lardelli M, Lendahl U** 1993 Motch A and motch B—two mouse Notch homologues coexpressed in a wide variety of tissues. Exp Cell Res 204:364–372
59. **Engin F, Yao Z, Yang T, Zhou G, Bertin T, Jiang MM, Chen Y, Wang L, Zheng H, Sutton RE, Boyce BF, Lee B** 2008 Dimorphic effects of Notch signaling in bone homeostasis. Nat Med 14:299–305
60. **Frenkel B, Capparelli C, Van Auken M, Baran D, Bryan J, Stein JL, Stein GS, Lian JB** 1997 Activity of the osteocalcin promoter in skeletal sites of transgenic mice and during osteoblast differentiation in bone marrow-derived stromal cell cultures: effects of age and sex. Endocrinology 138:2109–2116

The Endocrine Society. Downloaded from press.endocrine.org by [${individualUser.displayName}] on 21 January 2014. at 08:24 For personal use only. No other uses without permission. . All rights reserved.

61. **Kim JE, Nakashima K, de Crombrugghe B** 2004 Transgenic mice expressing a ligand-inducible cre recombinase in osteoblasts and odontoblasts: a new tool to examine physiology and disease of postnatal bone and tooth. Am J Pathol 165:1875–1882
62. **Pereira RM, Delany AM, Durant D, Canalis E** 2002 Cortisol regulates the expression of Notch in osteoblasts. J Cell Biochem 85:252–258
63. **Schnabel M, Fichtel I, Gotzen L, Schlegel J** 2002 Differential expression of Notch genes in human osteoblastic cells. Int J Mol Med 9:229–232
64. **Hilton MJ, Tu X, Wu X, Bai S, Zhao H, Kobayashi T, Kronenberg HM, Teitelbaum SL, Ross FP, Kopan R, Long F** 2008 Notch signaling maintains bone marrow mesenchymal progenitors by suppressing osteoblast differentiation. Nat Med 14:306–314
65. **Oldershaw RA, Tew SR, Russell AM, Meade K, Hawkins R, McKay TR, Brennan KR, Hardingham TE** 2008 Notch signaling through Jagged-1 is necessary to initiate chondrogenesis in human bone marrow stromal cells, but must be switched off to complete chondrogenesis. Stem Cells 26: 666–674
66. **Nofziger D, Miyamoto A, Lyons KM, Weinmaster G** 1999 Notch signaling imposes two distinct blocks in the differentiation of C2C12 myoblasts. Development 126:1689–1702

***Endocrinology* is published monthly by The Endocrine Society (http://www.endo-society.org), the foremost professional society serving the endocrine community.**

The Endocrine Society. Downloaded from press.endocrine.org by [${individualUser.displayName}] on 21 January 2014. at 08:24 For personal use only. No other uses without permission. . All rights reserved.